Grüneisen parameter of hcp-Fe to 171 GPa

Caitlin A. Murphy,[1] Jennifer M. Jackson,[1] Wolfgang Sturhahn,[2,3] and Bin Chen[1,4]

Received 2 September 2011; revised 3 November 2011; accepted 6 November 2011; published 20 December 2011.

[1] We measured the phonon density of states (DOS) of hexagonal close-packed iron (ε-Fe) with high statistical quality using nuclear resonant inelastic X-ray scattering and *in situ* X-ray diffraction experiments between pressures of 30 GPa and 171 GPa and at 300 K, with a neon pressure medium up to 69 GPa. The shape of the phonon DOS remained similar at all compression points, while the maximum (cutoff) energy increased regularly with decreasing volume. As a result, we present a generalized scaling law to describe the volume dependence of ε-Fe's total phonon DOS which, in turn, is directly related to the ambient temperature vibrational Grüneisen parameter (γ_{vib}). Fitting our individual γ_{vib} data points with $\gamma_{vib} = \gamma_{vib,0}(V/V_0)^q$, a common parameterization, we found an ambient pressure $\gamma_{vib,0} = 2.0 \pm 0.1$ for the range $q = 0.8$ to 1.2. We also determined the Debye sound velocity (v_D) from the low-energy region of the phonon DOS and our *in situ* measured volumes, and used the volume dependence of v_D to determine the commonly discussed Debye Grüneisen parameter (γ_D). Comparing our $\gamma_{vib}(V)$ and $\gamma_D(V)$, we found γ_{vib} to be ~10% larger than γ_D at any given volume. Finally, applying our $\gamma_{vib}(V)$ to a Mie-Grüneisen type relationship and an approximate form of the empirical Lindemann melting criterion, we predict the vibrational thermal pressure and estimate the high-pressure melting behavior of ε-Fe at Earth's core pressures. **Citation:** Murphy, C. A., J. M. Jackson, W. Sturhahn, and B. Chen (2011), Grüneisen parameter of hcp-Fe to 171 GPa, *Geophys. Res. Lett.*, *38*, L24306, doi:10.1029/2011GL049531.

1. Introduction

[2] Iron is thought to be the main constituent in the Earth's core [*McDonough*, 2003], and existing data suggest that hexagonal close-packed iron (ε-Fe) is the stable phase at core conditions [*Alfè et al.*, 2001; *Ma et al.*, 2004; *Dewaele et al.*, 2006; *Tateno et al.*, 2010]. Therefore, the accurate determination of ε-Fe's thermophysical properties is of fundamental importance for studies of the deep Earth. For example, accurate measurements of ε-Fe's thermodynamic Grüneisen parameter (γ_{th}) would aid in the determination of its high-pressure thermal equation of state, because γ_{th} is the coefficient that relates thermal pressure to thermal energy per unit volume. In addition, γ_{th} is used to reduce shock-compression data to isothermal data and to calculate adiabatic gradients [*Poirier*, 2000], both of which are important applications for furthering our understanding of Earth's core.

[3] The thermodynamic Grüneisen parameter is made up of electronic and vibrational components, the latter of which is directly related to the volume dependence of the phonon density of states (DOS). The vibrational Grüneisen parameter (γ_{vib}) of ε-Fe is particularly important because it is used to extrapolate available melting data to the inner core boundary, where Earth's solid inner core and liquid outer core are in contact. However, reported values of γ_{vib} are not in complete agreement [*Jeanloz*, 1979; *Brown and McQueen*, 1986; *Dubrovinsky et al.*, 2000; *Lübbers et al.*, 2000; *Alfè et al.*, 2001; *Anderson et al.*, 2001a, 2001b; *Ahrens et al.*, 2002; *Giefers et al.*, 2002; *Dewaele et al.*, 2006], and are often based on indirect or approximate determinations. As a result, uncertainty and confusion surround γ_{vib}, and a wide range of extrapolated melting temperatures have been reported.

[4] An approximate form of γ_{vib} is the Debye Grüneisen parameter (γ_D), which is based on Debye's approximation that the entire phonon DOS can be described by its low-energy region, where the dispersion relation is linear. In past studies, γ_D has been approximated from X-ray diffraction experiments via the Rietveld structural refinement method. From this refinement, one obtains an approximate mean-square atomic displacement and in turn, the Debye temperature, which is related to γ_D [*Dubrovinsky et al.*, 2000; *Anderson et al.*, 2001a, 2001b]. In addition, researchers have approximated γ_D from adiabatic decompression experiments via a thermodynamic relationship that relates γ and $(\partial T/\partial P)_S$ [*Boehler and Ramakrishnan*, 1980].

[5] Here we determine $\gamma_{vib}(V)$ from the total phonon DOS, which we measured at eleven compression points between pressures of 30 GPa and 171 GPa using nuclear resonant inelastic X-ray scattering (NRIXS) and *in situ* X-ray diffraction (XRD) experiments [*Sturhahn et al.*, 1995]. In addition, we determine $\gamma_D(V)$ for ε-Fe from the volume dependence of its Debye sound velocity, which we obtain from the low-energy region of the phonon DOS [*Sturhahn and Jackson*, 2007]. Our long NRIXS data-collection times and high-energy resolution produced the high statistical quality that is necessary to derive γ_{vib} and γ_D.

2. Experimental Procedure

[6] We prepared three modified panoramic diamond-anvil cells (DACs) with 90° openings on the downstream side and beveled anvils with flat culet diameters of 250 μm or 150 μm. A piece of 10 μm thick 95% enriched ^{57}Fe foil was loaded into beryllium gaskets with boron epoxy inserts, and a neon

[1]Seismological Laboratory, California Institute of Technology, Pasadena, California, USA.
[2]Advanced Photon Source, Argonne National Laboratory, Argonne, Illinois, USA.
[3]Now at Jet Propulsion Laboratory, Pasadena, California, USA.
[4]Now at Department of Geological Sciences, University of Michigan, Ann Arbor, Michigan, USA.

0094-8276/11/2011GL049531

Table 1. Experimental Results From NRIXS and *in Situ* XRD Measurements of ε-Fe[a]

V (cm^3/mol)	P (GPa)	C_{vib} (k_B/atom)	U_{vib} (meV/atom)	v_D (km/s)
5.92(2)[b]	30(2)	2.62(2)	43.9(5)	4.36(3)
5.81(1)[b]	36(2)	2.60(4)	44.3(9)	4.37(6)
5.56(1)[b]	53(3)	2.54(3)	45.2(6)	4.57(4)
5.36(1)[b]	69(4)	2.49(2)	46.0(5)	4.80(4)
5.27(2)	77(5)	2.47(2)	46.3(5)	4.93(3)
5.15(2)	90(5)	2.44(2)	46.8(6)	5.13(3)
5.00(2)[c]	106(6)	2.40(2)	47.5(4)	5.23(3)
4.89(2)[c]	121(8)	2.36(2)	48.2(4)	5.33(4)
4.81(2)[c]	133(8)	2.33(2)	48.6(5)	5.47(5)
4.70(2)[c]	151(9)	2.30(2)	49.1(6)	5.72(10)
4.58(2)[c]	171(11)	2.25(3)	50.0(9)	5.64(7)

[a]Volume (V) was measured with *in situ* XRD and converted to pressure (P) using the Vinet EOS [*Dewaele et al.*, 2006]; the vibrational specific heat capacity (C_{vib}) and vibrational energy (U_{vib}) per ^{57}Fe atom were determined from the integrated phonon DOS (equations (1) and (2)); and the Debye sound velocity (v_D) was obtained using the low-energy region of the measured phonon DOS and our *in situ* measured volumes, and accounts for ^{57}Fe enrichment levels. Values in parentheses give uncertainties for the last significant digit(s). Reported uncertainties for *Dewaele et al.*'s [2006] EOS parameters account for ~75% to 90% of the total pressure uncertainties.

[b]For these measurements, neon was loaded as the pressure transmitting medium.

[c]Texturing was observed at these compression points in the form of a loss of intensity in the (002) diffraction peak.

pressure transmitting medium was loaded for measurements made at atomic volumes of ε-Fe greater than 5.27 cm^3/mol ($P \leq 69$ GPa). For details of our DAC preparation, experimental procedures, and data analysis, see auxiliary material or *Murphy et al.* [2011].[1] The present analysis is performed on the dataset presented by *Murphy et al.* [2011], in addition to a recently acquired higher-pressure point (V = 4.58 ± 0.02 cm^3/mol, P = 171 ± 11 GPa). We note that results from the analysis presented by *Murphy et al.* [2011] with the addition of this new largest compression point agree with the original results within uncertainty.

[7] From our *in situ* XRD experiments, we obtained the atomic volume (V) of our sample at each of our eleven compression points. To derive γ_{vib} and γ_D, we rely on these *in situ* measured volumes. To present our results on a common scale and for discussion, we convert our measured volumes to pressures using the Vinet equation of state (EOS) [*Dewaele et al.*, 2006] (Table 1).

[8] From our NRIXS experiments, we obtained ε-Fe's total phonon DOS, $D(E, V)$ [*Sturhahn*, 2000; *Sturhahn and Jackson*, 2007], from which we directly determined two parameters that relate γ_{vib} to the vibrational thermal pressure via a Mie-Grüneisen type relationship. The vibrational component of the specific heat capacity per ^{57}Fe atom (C_{vib}) is given by

$$C_{vib}(V) = k_B \int \left(\frac{\beta E}{2\sinh(\beta E/2)}\right)^2 D(E,V)\mathrm{d}E, \qquad (1)$$

and the vibrational energy per ^{57}Fe atom (U_{vib}) is given by

$$U_{vib}(V) = \frac{1}{2}\int E \coth\frac{\beta E}{2} D(E,V)\mathrm{d}E \qquad (2)$$

(Table 1), where k_B is Boltzmann's constant and β is the inverse temperature [*Sturhahn*, 2004].

3. Vibrational Grüneisen Parameter

[9] Qualitative inspection of our data reveals that our phonon DOS are similar in shape at all compression points, and that any pair of phonon DOS appears to be related by a single overall scaling parameter. This suggestion can be evaluated in Figure 1, where we plot our measured phonon DOS at each compression point in black, along with the phonon DOS at V_i = 5.15 ± 0.02 cm^3/mol (P = 90 ± 5 GPa) that has been scaled using

$$D(E,V) = \xi(V/V_i)\cdot D[\xi(V/V_i)\cdot E, V_i] \qquad (3)$$

and the appropriate scaling parameter (ξ) for each pair of phonon DOS in green. We note that ξ is energy-independent and $\xi(1) = 1$.

[10] To determine the appropriate scaling parameter for each pair of phonon DOS, we assign one spectrum to be an initial reference phonon DOS, $D(E, V_i)$, to which we apply equation (3). We then minimize the least-squares difference between this scaled reference phonon DOS and each of the other ten unscaled phonon DOS, $D(E, V_j)$ (Figure 1). This process is repeated with each phonon DOS serving as the reference, resulting in eleven datasets that each contain ten data points. To incorporate our entire scaling parameter

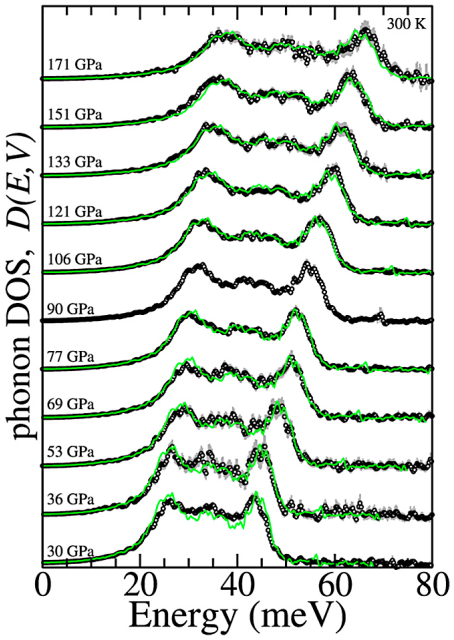

Figure 1. Comparison of measured and scaled phonon DOS of ε-Fe. Black open circles show the measured phonon DOS at each compression point with uncertainties; green curves show the phonon DOS at V_i = 5.15 ± 0.02 cm^3/mol (P = 90 ± 5 GPa), scaled to each other measured phonon DOS using equation (3) and the appropriate scaling parameter for each pair of phonon DOS, following the procedure described in section 3.

[1]Auxiliary materials are available in the HTML. doi:10.1029/2011GL049531.

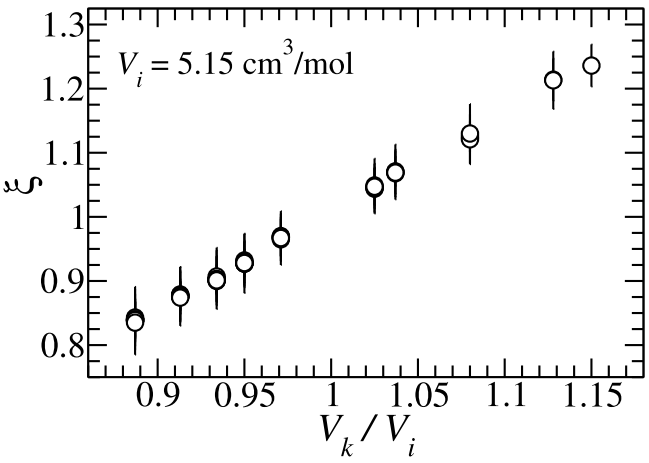

Figure 2. A demonstration of our scaling parameter analysis for ε-Fe's phonon DOS. The scaling parameter (ξ) is plotted as a function of the relative volumes of a scaled reference phonon DOS, $D(E, V_i)$, and all other unscaled phonon DOS, (E, V_k). In this example, $V_i = 5.15 \pm 0.02$ cm^3/mol ($P = 90 \pm 5$ GPa). All scaling analysis data have been included, following equation (4).

analysis into each dataset, we then rescale all of our data to each reference volume (V_i) by

$$\xi\left(\frac{V_k}{V_i}\right) = \xi\left(\frac{V_k}{V_j}\right) \cdot \xi\left(\frac{V_j}{V_i}\right). \tag{4}$$

[11] In Figure 2, we show the result of this scaling analysis for an example reference phonon DOS: $\xi(V_k/V_i)$ for $V_i = 5.15 \pm 0.02$ cm^3/mol. Given the smooth trend and small errors, we find that a generalized scaling law successfully describes the volume dependence of ε-Fe's phonon DOS. We note that a similar analysis was previously performed by *Alfè et al.* [2001], who investigated the volume dependence of dispersion curves for ε-Fe using *ab initio* density-functional theory (DFT) calculations. *Alfè et al.* [2001] reported $\xi(1.244) = 1.409$ for $V_i = 4.20$ cm^3/mol, which agrees fairly well with the value predicted by extrapolating our results to the same volume ratio. However, this comparison is largely qualitative because *Alfè et al.*'s [2001] scaling parameter was determined for dispersion curves calculated at $T = 4000$ K, and $V_i = 4.20$ cm^3/mol is beyond the compression range of our measurements.

[12] Finally, we derive an expression for the relationship between γ_{vib} and the volume dependence of the scaling parameter, $\xi(V/V_i)$, by combining the commonly used parameterization

$$\gamma_{vib} = \gamma_{vib,i}\left(\frac{V}{V_i}\right)^q, \tag{5}$$

with the definition of the vibrational Grüneisen parameter

$$\gamma_{vib} = \frac{\partial \ln \xi(V/V_i)}{\partial \ln V_i}, \tag{6}$$

where $\gamma_{vib,i}$ and V_i are the vibrational Grüneisen parameter and volume at a reference compression, and q is a fitting parameter. Substituting equation (5) into equation (6) and integrating, we obtain

$$\xi\left(\frac{V}{V_i}\right) = \xi_i \exp\left\{\frac{\gamma_{vib,i}}{q}\left[\left(\frac{V}{V_i}\right)^q - 1\right]\right\} \tag{7}$$

when $q \neq 0$. At the reference compression, $V = V_i$ and $\xi_i = \xi(1) = 1$, so equation (7) simplifies to

$$\xi\left(\frac{V}{V_i}\right) = \exp\left(\frac{-\gamma_{vib,i}}{q}\right)\exp\left\{\frac{\gamma_{vib,i}}{q}\left(\frac{V}{V_i}\right)^q\right\}. \tag{8}$$

[13] Fitting each of our eleven $\xi(V_k/V_i)$ datasets with equation (8) and allowing both $\gamma_{vib,i}$ and q to vary freely, we found large uncertainties in q, with the most tightly constrained fit being $q(5.15$ cm^3/mol$) = 0.8 \pm 0.7$. Therefore, we re-performed the fits with q fixed to one of three assigned values: first, $q(5.15$ cm^3/mol$) = 0.8$; second, the commonly assumed $q = 1$; and third, $q = 1.2$. Finally, we fit the resulting three sets of $\gamma_{vib,i}(V_i)$ with equation (5) and obtained ambient pressure $\gamma_{vib,0} = 1.88 \pm 0.02$ for $q = 0.8$; $\gamma_{vib,0} = 1.98 \pm 0.02$ for $q = 1.0$; and $\gamma_{vib,0} = 2.08 \pm 0.02$ for $q = 1.2$. These results can be combined and presented as $\gamma_{vib,0} = 2.0 \pm 0.1$, where we assign the error to reflect fitting parameter uncertainties and the range associated with our fixed q values.

4. Debye Grüneisen Parameter

[14] The low-energy region of a material's phonon DOS is related to its Debye sound velocity (v_D), provided it is parabolic ("Debye-like"). We determined v_D for ε-Fe at each of our eleven compression points (Table 1) by using an exact relation for the dispersion of low-energy acoustic phonons with our *in situ* measured volumes, and determining the best energy range to use for this fit [see *Sturhahn and Jackson*, 2007, equation 9]. The large compression range and high statistical quality of our data allow us to calculate a very accurate $v_D(V)$, which is related to γ_D by

$$\gamma_D = \frac{1}{3} - \frac{V}{v_D}\left(\frac{\partial v_D}{\partial V}\right)_T. \tag{9}$$

[15] Combining equations (9) and (5) and integrating, we obtain the expression

$$v_D = v_{D,0}\left(\frac{V}{V_i}\right)^{1/3}\exp\left\{-\frac{\gamma_{D,0}}{q}\left[\left(\frac{V}{V_0}\right)^q - 1\right]\right\}, \tag{10}$$

which depends on the ambient pressure Debye sound velocity ($v_{D,0}$), Debye Grüneisen parameter ($\gamma_{D,0}$), and volume (V_0) [*Dewaele et al.*, 2006], and the fitting parameter q [*Sturhahn and Jackson*, 2007]. Therefore, to determine $\gamma_D(V)$, we fit our $v_D(V_i)$ with equation (10), fixing q as in section 3, and found $\gamma_{D,0} = 1.70 \pm 0.07$ and $v_{D,0} = 3.66 \pm 0.06$ km/s for $q = 0.8$; $\gamma_{D,0} = 1.78 \pm 0.07$ and $v_{D,0} = 3.63 \pm 0.06$ km/s for $q = 1.0$; and $\gamma_{D,0} = 1.87 \pm 0.08$ and $v_{D,0} = 3.60 \pm 0.06$ km/s for $q = 1.2$. Combining these results as in section 3, we find $\gamma_{D,0} = 1.8 \pm 0.1$ and $v_{D,0} = 3.63 \pm 0.09$ km/s.

5. Discussion

[16] A generalized scaling law describes the volume dependence of ε-Fe's phonon DOS fairly well. However,

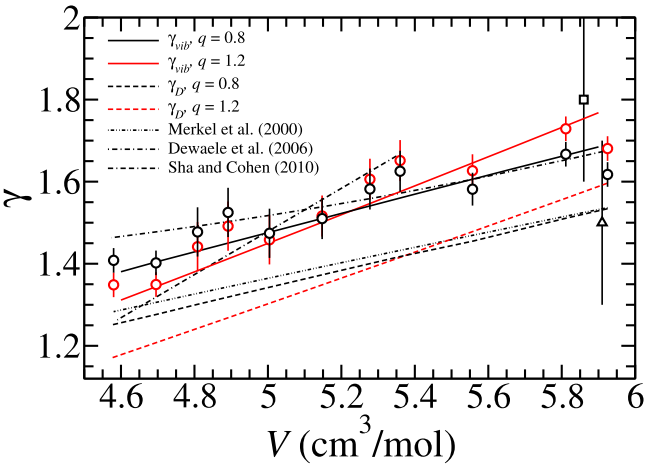

Figure 3. Grüneisen parameter of ε-Fe. Individual $\gamma_{vib,i}$ from section 3 are plotted as circles for q = 0.8 (black) and q = 1.2 (red); fitted curves of $\gamma_{vib,i}$ with equation (5) (solid lines) and $\gamma_D(V)$ (dashed lines) are shown for q = 0.8 (black lines) and q = 1.2 (red lines). The dash-dotted line shows *Dewaele et al.*'s [2006] $\gamma_D(V)$, based in part on their XRD data; the black square and triangle show the individual γ_D determined from NRIXS measurements by *Lübbers et al.* [2000] and *Giefers et al.* [2002], respectively, at the average volume of each experimental pressure range; the dash-dot-dotted line shows *Merkel et al.*'s [2000] $\gamma_{th}(V)$, determined from Raman spectroscopy experiments; and the dash-dash-dotted line shows *Sha and Cohen*'s [2010] γ_{th}, based on the results of their DFT calculations at T = 500 K, given in their Figure 8.

it is important to note that the relative intensity of the middle vibrational mode decreases with respect to the low- and high-energy vibrational modes with compression (Figure 1). This slight deviation from perfectly generalized scaling could contribute to the poorly constrained nature of q, which is the parameter that controls the rate at which γ_{vib} and γ_D decrease with decreasing volume.

[17] Our $\gamma_{vib,i}$ and γ_D at each compression point are listed in Table S1 in the auxiliary material, and are plotted with their fitted curves in Figure 3. We find that γ_{vib} is systematically ~10% larger than γ_D, which may be explained in part by the fact that γ_{vib} is derived from the entire phonon DOS, while γ_D depends only on the acoustic regime (i.e., the low-energy region). There is not enough information to determine whether this discrepancy is related to sample texturing, which we observed in our five largest compression points (see auxiliary material).

[18] Our $\gamma_{vib}(V)$ for q = 0.8 agree fairly well with *Anderson et al.*'s [2001a, 2001b] $\gamma_v(V)$, determined from intensity changes in static-compression XRD lines with compression. In addition, the slope for q = 0.8 agrees fairly well with that of *Dewaele et al.*'s [2006] $\gamma_D(V)$, which was determined from a combination of previously reported shock-compression data, an assumed volume dependence of γ, and their static-compression XRD experiments. However, *Dewaele et al.*'s [2006] $\gamma_D(V)$ is ~10% larger than our $\gamma_D(V)$. Finally, two previous NRIXS experiments on ε-Fe reported volume-independent γ_D up to 42 GPa; our $\gamma_D(V)$ agree well with *Giefers et al.*'s [2002] γ_D, but are significantly lower than *Lübbers et al.*'s [2000] γ_D (Figure 3).

[19] Although γ_{vib} is only one component of the total γ_{th}, we compare our results with reported values for ε-Fe's $\gamma_{th}(V)$. *Merkel et al.* [2000] used Raman spectroscopy experiments to determine γ_0 = 1.68 ± 0.2 for q = 0.7 ± 0.5, which is very similar to our $\gamma_D(V)$ for q = 0.8. *Sha and Cohen* [2010] performed DFT calculations to find $\gamma_{th}(V)$ for nonmagnetic ε-Fe at 500 K. Their result agrees fairly well with our high-pressure $\gamma_{vib,i}$ but has a steeper slope than our fitted curves, possibly due to different EOS parameters (Figure 3). Finally, *Brown and McQueen* [1986] found γ = 1.56 at a density of 12.54 g/cm^3 using shock-compression experiments, which is larger than our predicted value at the same density (~1.3). However, we note that the *Brown and McQueen* [1986] data point is for liquid iron, whereas our results are for solid ε-Fe at 300 K.

[20] To explore the geophysical applications of γ_{vib}, we first investigate the volume-dependent vibrational thermal pressure (P_{vib}) of ε-Fe by applying our $\gamma_{vib}(V)$ to a Mie-Grüneisen type relationship:

$$P_{vib} = \left(\frac{C_{vib}\gamma_{vib}}{C_{vib} + C_{el}}\right)\frac{U_{vib}}{V}. \quad (11)$$

$C_{vib}(V)$ and $U_{vib}(V)$ are obtained from our measurements (equations (1) and (2)), and we use approximate values for the electronic component of the specific heat capacity (C_{el}) from *Alfè et al.* [2001]. Applying these values and our $\gamma_{vib}(V)$ to equation (11), we find P_{vib}(300 K) = 2.39 ± 0.08 GPa and 2.75 ± 0.1 GPa at our smallest (30 GPa) and largest (171 GPa) compression points, respectively. Reported errors account for the previously mentioned uncertainties in γ_{vib} and our measured uncertainties in V, C_{vib}, and U_{vib}. These values agree very well with our P_{vib} calculated directly from the integrated phonon DOS [*Murphy et al.*, 2011], which were 2.31 ± 0.06 GPa and 2.74 ± 0.06 GPa at our smallest and largest compression points. Finally, accounting for electronic and anharmonic contributions at high-temperatures following *Murphy et al.* [2011], we find the total thermal pressure (P_{th}) of ε-Fe at our new, largest compression point (V = 4.58 cm^3/mol) to be P_{th}(2000 K) = 16 GPa, P_{th}(4000 K) = 37 GPa, and P_{th}(5600 K) = 56 GPa.

[21] Next, we use our $\gamma_{vib}(V)$ to estimate the high-pressure melting behavior of ε-Fe by applying it to a commonly used, approximate form of the empirical Lindemann melting criterion

$$T_M(V) = T_M^{ref}\left(\frac{V}{V_M^{ref}}\right)^{2/3}\exp\left\{\frac{2\gamma_{vib}^{ref}}{q}\left[1 - \left(\frac{V}{V_M^{ref}}\right)^q\right]\right\}, \quad (12)$$

where T_M^{ref}, V_M^{ref}, and γ_{vib}^{ref} are the melting temperature, volume, and vibrational Grüneisen parameter at a reference melting point. We take the melting point measured by *Ma et al.* [2004] using laser-heated synchrotron X-ray diffraction experiments as the reference: T_M^{ref} = 3510 ± 100 K at $P_{300\ K}$ = 105 GPa, or V_M^{ref} = 5.01 cm^3/mol using the Vinet EOS [*Dewaele et al.*, 2006]. From equation (5) and our results in section 3, we find γ_{vib}^{ref} = 1.47 ± 0.1. Applying these reference point values to equation (12), we estimate T_M(4.70 cm^3/mol) = 4100 ± 100 K and T_M(4.58 cm^3/mol) = 4300 ± 100 K for ε-Fe. We note that replacing γ_{vib}^{ref} with γ_D^{ref} = 1.32 ± 0.1 (see section 4) results in melting temperatures that are ~3% smaller at these compressions.

[22] Finally, we account for thermal pressure at the melting temperatures of our two largest compression points following *Murphy et al.* [2011], which gives P_{th}(4.70 cm^3/mol, 4100 K) = 38 GPa and P_{th}(4.58 cm^3/mol, 4300 K) = 40 GPa, respectively. Applying the corresponding thermal pressure correction assuming constant volume, we find T_M(186 GPa) = 4100 ± 100 K and T_M(208 GPa) = 4300 ± 100 K. These estimated melting points agree very well with our previously reported high-pressure melting behavior of ε-Fe, determined from the mean-square displacement of ^{57}Fe atoms which we obtained directly from the integrated phonon DOS [*Murphy et al.*, 2011].

[23] **Acknowledgments.** We would like to thank D. Zhang, H. Yavas, and J.K. Wicks for assistance during the experiments, and NSF-CAREER-0956166 and Caltech for support of this research. We thank two anonymous reviewers for their comments that helped to improve our manuscript. Use of the Advanced Photon Source was supported by the U.S. D.O.E., O.S., O.B.E.S. (DE-AC02-06CH11357). Sector 3 operations and the GSE-CARS gas-loading facility are supported in part by COMPRES (NSF EAR 06-49658).

[24] The Editor thanks two anonymous reviewers for their assistance in evaluating this paper.

References

Ahrens, T. J., K. G. Holland, and G. Q. Chen (2002), Phase diagram of iron, revised-core temperatures, *Geophys. Res. Lett.*, *29*(7), 1150, doi:10.1029/2001GL014350.

Alfè, D., G. D. Price, and M. J. Gillan (2001), Thermodynamics of hexagonal-close-packed iron under Earth's core conditions, *Phys. Rev. B*, *64*(4), 045123, doi:10.1103/PhysRevB.64.045123.

Anderson, O. L., L. Dubrovinsky, S. K. Saxena, and T. LeBihan (2001a), Experimental vibrational Grüneisen ratio values for ε-iron up to 330 GPa at 300 K, *Geophys. Res. Lett.*, *28*(2), 399–402, doi:10.1029/2000GL008544.

Anderson, O. L., L. Dubrovinsky, S. K. Saxena, and T. LeBihan (2001b), Correction to "Experimental vibrational Grüneisen ratio values for ε-iron up to 330 GPa at 300 K," *Geophys. Res. Lett.*, *28*(12), 2359, doi:10.1029/2001GL013085.

Boehler, R., and J. Ramakrishnan (1980), Experimental results on the pressure dependence of the Grüneisen Parameter: A review, *J. Geophys. Res.*, *85*(B12), 6996–7002, doi:10.1029/JB085iB12p06996.

Brown, J. M., and R. G. McQueen (1986), Phase transitions, Grüneisen parameter, and elasticity for shocked iron between 77 GPa and 400 GPa, *J. Geophys. Res.*, *91*(B7), 7485–7494, doi:10.1029/JB091iB07p07485.

Dewaele, A., P. Loubeyre, F. Occelli, M. Mezouar, P. I. Dorogokupets, and M. Torrent (2006), Quasihydrostatic equation of state of iron above 2 Mbar, *Phys. Rev. Lett.*, *97*(21), 215504, doi:10.1103/PhysRevLett.97.215504.

Dubrovinsky, L. S., S. K. Saxena, N. A. Dubrovinskaia, S. Rekhi, and T. LeBihan (2000), Grüneisen parameter of epsilon-iron up to 300 GPa from in-situ X-ray study, *Am. Mineral.*, *85*(2), 386–389.

Giefers, H., R. Lübbers, K. Rupprecht, G. Wortmann, D. Alfè, and A. I. Chumakov (2002), Phonon spectroscopy of oriented hcp iron, *High Pressure Res.*, *22*(2), 501–506, doi:10.1080/08957950212817.

Jeanloz, R. (1979), Properties of iron at high pressures and the state of the core, *J. Geophys. Res.*, *84*(B11), 6059–6069, doi:10.1029/JB084iB11p06059.

Lübbers, R., H. F. Grünsteudel, A. I. Chumakov, and G. Wortmann (2000), Density of phonon states in iron at high pressure, *Science*, *287*(5456), 1250–1253, doi:10.1126/science.287.5456.1250.

Ma, Y. Z., M. Somayazulu, G. Shen, H. K. Mao, J. F. Shu, and R. J. Hemley (2004), In situ X-ray diffraction studies of iron to Earth-core conditions, *Phys. Earth Planet. Inter.*, *143–144*, 455–467, doi:10.1016/j.pepi.2003.06.005.

McDonough, W. F. (2003), Compositional model for the Earth's core, in *Treatise on Geochemistry*, vol. 2, *The Mantle and Core*, edited by D. H. Heinrich and K. T. Karl, pp. 547–568, Pergamon, Oxford, U. K., doi:10.1016/B0-08-043751-6/02015-6.

Merkel, S., A. F. Goncharov, H. K. Mao, P. Gillet, and R. J. Hemley (2000), Raman spectroscopy of iron to 152 gigapascals: Implications for Earth's inner core, *Science*, *288*(5471), 1626–1629, doi:10.1126/science.288.5471.1626.

Murphy, C. A., J. M. Jackson, W. Sturhahn, and B. Chen (2011), Melting and thermal pressure of hcp-Fe from the phonon density of states, *Phys. Earth Planet. Inter.*, *188*(1–2), 114–120, doi:10.1016/j.pepi.2011.07.001.

Poirier, J.-P. (2000), *Introduction to the Physics of the Earth's Interior*, 2nd ed., pp. 232–233, Cambridge Univ. Press, Cambridge, U. K.

Sha, X. W., and R. E. Cohen (2010), First-principles thermal equation of state and thermoelasticity of hcp Fe at high pressures, *Phys. Rev. B*, *81*(9), 094105, doi:10.1103/PhysRevB.81.094105.

Sturhahn, W. (2000), CONUSS and PHOENIX: Evaluation of nuclear resonant scattering data, *Hyperfine Interact.*, *125*(1/4), 149–172, doi:10.1023/A:1012681503686.

Sturhahn, W. (2004), Nuclear resonant spectroscopy, *J. Phys. Condens. Matter*, *16*(5), S497–S530, doi:10.1088/0953-8984/16/5/009.

Sturhahn, W., and J. M. Jackson (2007), Geophysical applications of nuclear resonant spectroscopy, *Spec. Pap. Geol. Soc. Am.*, *421*, 157–174.

Sturhahn, W., T. S. Toellner, E. E. Alp, X. Zhang, M. Ando, Y. Yoda, S. Kikuta, M. Seto, C. W. Kimball, and B. Dabrowski (1995), Phonon density of states measured by inelastic nuclear resonant scattering, *Phys. Rev. Lett.*, *74*(19), 3832–3835, doi:10.1103/PhysRevLett.74.3832.

Tateno, S., K. Hirose, Y. Ohishi, and Y. Tatsumi (2010), The structure of iron in Earth's inner core, *Science*, *330*(6002), 359–361, doi:10.1126/science.1194662.

B. Chen, Department of Geological Sciences, University of Michigan, 1100 N. University Ave., Ann Arbor, MI 48109, USA.

J. M. Jackson and C. A. Murphy, Seismological Laboratory, California Institute of Technology, M/C 252-21, Pasadena, CA 91125, USA. (caitlinm@caltech.edu)

W. Sturhahn, Jet Propulsion Laboratory, 4800 Oak Grove Dr., Pasadena, CA 91109, USA.